Correction of Dynamic Multipoles for APPLE-II Undulator with Flat Wires

Y. Kikuchi[1], M. Hosaka[1], N. Yamamoto[1], Y. Takashima[1], M. Adachi[2], H. Zen[2] and M. Katoh[2]
[1]*Graduate School of Engineering, Nagoya University, Nagoya 464-8603, Japan*
[2] *UVSOR Facility, Institute for Molecular Science, Okazaki 444-8585, Japan*

Introduction

APPLE-II undulator can produce quasi-monochromatic light of variable polarization though its magnetic circuit is relatively simple. Therefore, it has been installed in many synchrotron radiation facilities and will be installed in Central Japan Synchrotron Radiation Research Facility under construction in Aichi prefecture.

APPLE-II undulator also has been installed in UVSOR-II electron storage ring [1]. When the undulator is operated in vertical polarization mode with narrower gap than 40 mm, the lifetime of electron beam circulating in the storage ring significantly decreases. The reason is considered as dynamic multipole kicks in the undulator, which strongly depends on the undulator gap. At UVSOR-II, multi-wires [2], which are glued in the upper and lower surface of undulator beam duct, are candidate to compensate the multipole effects. In order to evaluate the validity of this method, we numerically studied the dynamic multipoles of the undulator and experimentally examined the correction capability of multi-wires.

Numerical Study on Dynamic Multipoles

In order to evaluate dynamic multipoles generated in the undulator operated in vertical polarization mode, we calculated the relation between the horizontal beam injection point x and the horizontal beam angle in undulator terminus x' using a 3D magnetostatic code RADIA [3]. The result is shown in Fig.1. The quadrupole magnetic field is strong within x = ±5 mm and the higher order multipole magnetic field is strong in the other range. Expected multipole kick with multi-wire correction is also shown in Fig.1 as red line. Since the amplitude of multipole kick is comparative with that of 40-mm-gap condition, we expected significant improvement of the electron beam lifetime with the correction method.

Experimental Examination

Multi-wires were installed in APPLE-II undulator in UVSOR-II (Fig. 2) and we tested the effect of multipole correction on the beam lifetime. The result is shown in Table 1. When the multipoles were corrected by the multi-wires, the electron beam lifetime is significantly improved than that without correction. This multi-wires will enables us to use the undulator with vertical and narrow gap condition. Such operational condition is quite important for angle-resolved photoelectron spectroscopy application of APPLE-II undulator.

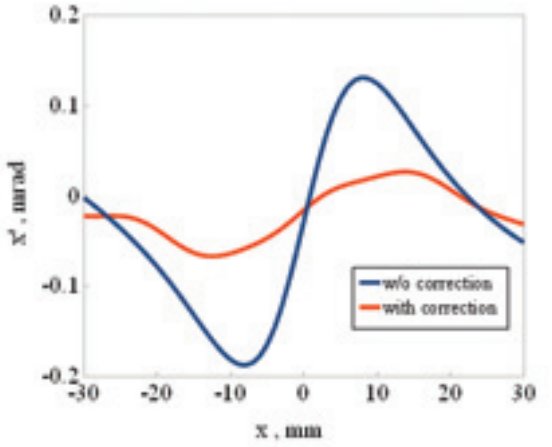

Fig. 1. The relation between x and x', when the undulator gap is operated with 30 mm gap and vertical polarization mode. (Blue:Without correciton, Red:With correction).

Fig. 2. Multi-wires installed in APPLE-II undulator.

Table 1. Result of correction of multipole field with multi-wires.

Gap [mm]	Beam liftime [mA hr]	
	W/o correction	With correction
100	300	—
30	100	290

[1] UVSOR Activity Report **37** (2010) 12.
[2] J. Bahrdt *et al.*, Proceedings of EPAC08 (2008) 2222.
[3] P. Elleaume *et al.*, Proceedins of PAC97 (1997) 3509.

Laser-Power-Dependence of Coherent THz Radiation from Electron Bunches Circulating in a Storage Ring

N. Yamamoto[1], M. Shimada[2], M. Adachi[3,4], H. Zen[3,4], T. Tanikawa[4], Y. Taira[1], S. Kimura[3,4], M. Hosaka[1], Y. Takashima[1], T. Takahashi[5] and M. Katoh[3,4]

[1]*Graduate School of Engineering, Nagoya University, Nagoya 464-8603, Japan*
[2]*High Energy Accelerator Research Organization, KEK, Tsukuba 305-0801, Japan*
[3]*UVSOR Facility, Institute for Molecular Science, Okazaki 444-8585, Japan*
[4]*School of Physical Sciences, The Graduate University for Advanced Studies (SOKENDAI), Okazaki 444-8585, Japan*
[5]*Research Reactor Institute, Kyoto University, Kumatori 590-0494, Japan*

Introduction

In order to study in detail the formation of the micro-structure in electron bunches, we have performed laser slicing experiments at the UVSOR-II electron storage ring. Coherent synchrotron radiation (CSR) in the THz region, which contains information on the micro-structure, was observed under various laser energies.

Experiments

The intensity of the THz light was measured by an InSb hot-electron bolometer (QMC, QFI/2) and the spectrum was analyzed at the IR/THz beamline (BL6B) using an in-vacuum Martin–Puplett interferometer (JASCO, FARIS-1), which was used to measure the spectra in the 2–50 cm^{-1} range with a resolution of 1 cm^{-1}. Pulse processing for the CSR measurement was done using a gated integrator (SRS, SR250) to reduce the back ground from normal SR. The gated integrator was triggered by a 1-kHz repetition signal of the laser system, and a width of about 5 μs was chosen. In our measurements, the THz light intensity was evaluated to be 10^4–10^5 times larger than that of normal SR.

Results and Discussion

CSR spectra shown in Fig. 1 were taken for four different laser energies —2.0, 1.5, 1.0, and 0.5 mJ— with same laser pulse duration of 322 fs. The measured spectra are divided by that of normal SR in order to exclude the sensitivity dependence of the bolometer. Each spectrum has two peaks in different frequency ranges. The peaks in the higher and lower frequencies correspond to CSRs emitted in the first turn and in the second turn of the storage ring. Since the temporal resolution of the detector is about 1 μs and the spectra were time-averaged, it cannot resolve the emission from each turn. The measured double peak can be explained as a multi-turn effect [1].

As the laser energy increases, especially for the peak in the higher frequency range, the peaks shift to the lower frequency component increases gradually. The difference in spectral shape with different laser energies arises from the growth of the micro-structure in electron bunches. The dip structure becomes larger and wider as the laser energy increases, and this leads to an increase in the lower-frequency components.

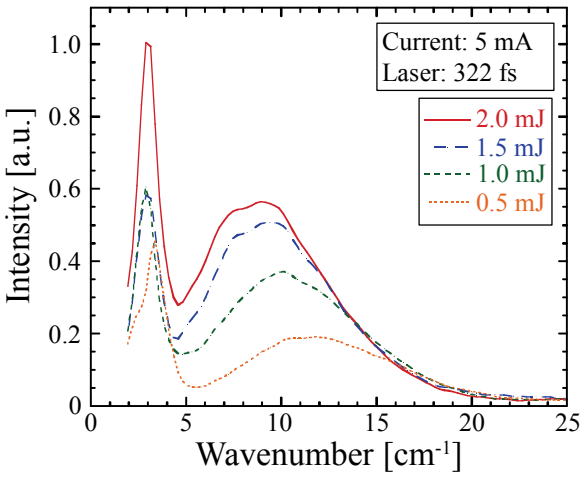

Fig. 1. THz CSR spectra with different energies of slicing laser pulse introduced.

Conclusions

The formation of micro-structure in electron bunches by the laser slicing technique was experimentally studied. The THz CSR spectra were measured for various laser energies. The measured spectra have double-peak structure, which can be attributed to the contributions of the first and second turns. The spectral shape depends strongly on the laser parameters.

The THz CSR spectra were compared with numerical calculations. The spectral shapes agree with the numerical calculations qualitatively, but some discrepancies in the wave number remains. Details of those results are described in Ref. [2].

[1] M. Shimada, *et. al.*, Phys. Rev. Lett. **103** (2009) 144802
[2] N. Yamamoto, *et. al.*, Nuclear Instruments and Methods in Physics Research A, in press.

Practical Introduction of Vertical Beam Position Feedback System

H. Zen[1], K. Hayashi[1], M. Adachi[1], N. Yamamoto[2], J. Yamazaki[1] and M. Katoh[1]
[1]*UVSOR Facility, Institute for Molecular Science, Okazaki 444-8585, Japan*
[2]*Graduate School of Engineering, Nagoya University, Nagoya 464-8603, Japan*

Introduction

In 2008, an orbit feedback system was developed for stabilizing the vertical electron beam position in the UVSOR-II storage ring [1]. Then, it was confirmed that the feedback system could suppress the slow drift of the vertical beam position. In this fiscal year, we have introduced the feedback system to user operations with a modification of the system.

Feedback System

The feedback system consists of 24 Beam Position Monitors (BPMs), 16 Steering Magnets (SMs) and control PCs. Firstly, the electron beam orbit was measured by the BPMs, which measures the beam position at 24 points of the ring. Secondly, control PCs calculates the applicable strength of SMs, which minimizes the displacement of orbit. Finally, strength of SMs is changed according to the calculated values. This system minimizes the displacement of electron beam along the storage ring.

Result of Test Operation

During night operations, usually done from Thursday night to Friday morning, we carried out some test operations of the orbit feedback system before introducing the system to normal user operation. A result of test operation is shown in Fig. 1. We found that the feedback system caused sudden orbit change shown in Fig. 1. At the same time, sudden intensity change of synchrotron radiation was observed in user beamlines. The origin of sudden orbit change was determined as a lack of resolution of SMs, whose minimum variation of the beam position is around 4 μm. Therefore, we made a modification on the system to have higher resolution.

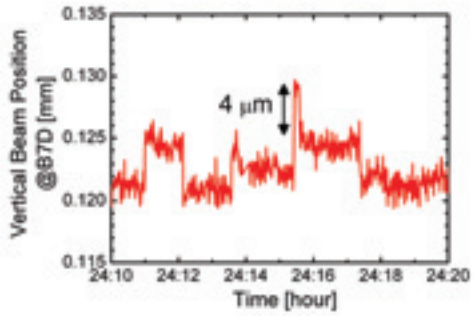

Fig. 1. Temporal evolution of vertical beam position during a test operation of the orbit feedback system.

Improvements

To improve the resolution, we newly added 100-turn coils to outside of the SMs. And for the power supply of the additional coil, DC power supplies (KIKUSUI, PMC-18-2A) were introduced. We also installed a 12 bit ADC board (INTERFACE, PCI-3341A) for controlling the new power supplies. The achieved resolution of the beam position with the improved system is around 0.15 μm. After installation, it was confirmed that the improved system did not make sudden orbit change.

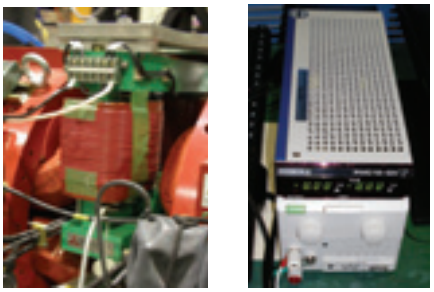

Fig. 2. Photographs of additional equipments. Left: Additional small coil around the steering magnet. Right: Remotely controllable DC power supply.

Introduction to User Operation

The improved orbit stabilization system has been introduced to user operations since December 2010. A typical temporal evolution of the vertical beam position during 36-hour operation is shown in Fig. 3. As shown in the figure, the drift of vertical beam position is drastically suppressed by the feedback control. And the orbit feedback system may contribute to suppress the photon energy variation in user beamlines and to achieve higher reproducibility of user experiments.

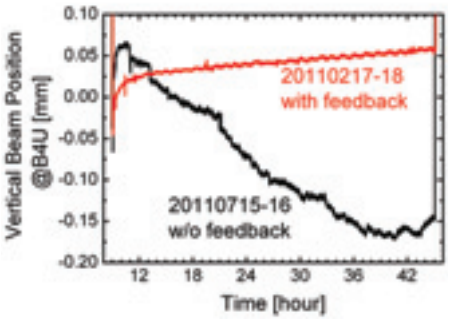

Fig. 3. Temporal evolution of vertical electron beam position at the downstream of bending magnet No. 4.

[1] Y. Suzuki *et al.*, UVSOR Activity Report **36** (2009) 32.

Stabilization of the Accelerated Charge of UVSOR-II Injector

H. Zen, K. Hayashi, J. Yamazaki, M. Adachi and M. Katoh
UVSOR Facility, Institute for Molecular Science, Okazaki 444-8585, Japan

Introduction

In fiscal year 2009, a stabilization system for injection septum of UVSOR-II booster synchrotron has been developed [1]. By using the system, the stability of accelerated charge in the synchrotron was drastically improved. However, we found another source of fluctuation of the accelerated charge, which was fluctuation of the RF power fed to the linac of UVSOR-II injector. In this fiscal year, we added feed-forward system for stabilizing the accelerated charge of the injector.

Principle of Stabilization Method

The energy gain of an RF Linac can be described in the formula,

$$\delta E_{\mathrm{kin}} = A\sqrt{P_0} - BI_{\mathrm{b}}\,, \qquad (1)$$

where δE_{kin} is the energy gain, P_0 is the fed power to the linac, I_{b} is the averaged electron beam current injected to the Linac, A and B are constant. The best way to stabilize the energy gain is stabilize the fed power and beam current. However, we don't have remote control for the fed power. Thus we decided to vary the averaged beam current for stabilizing the energy gain.

Feed-Forward System

The schematic diagram of developed feed-forward system is shown in Fig. 1. In this system, strength of the solenoid coil between the electron gun and linac is used for changing the average beam current (I_{b}) injected to the linac. Amplitude of fed RF power (P_0) to the linac is measured with an RF detector and an oscilloscope. The measured waveform is sent to control PC, which determines the optimum excitation current of solenoid coil from a look-up table or an equation.

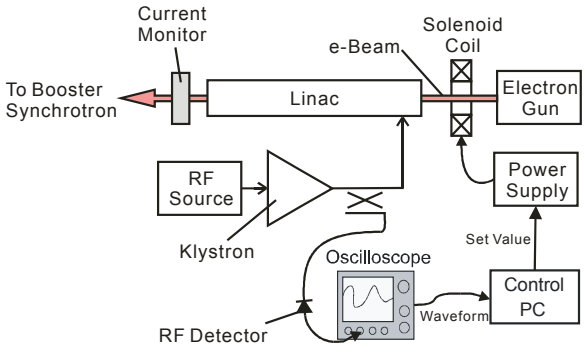

Fig. 1. Schematic diagram of feed-forward system.

The relationship between the measured RF power and the optimum excitation current of solenoid coil was experimentally obtained. It was found that the optimum current had quadratic dependence on the measured RF power.

Results

The results of 12-hour top-up operation are shown in Figs. 2. According to the changes of RF power fed to the Linac, the excitation current of the solenoid coil was controlled as shown in Fig. 2 (a). Then the accelerated charge in the booster synchrotron was kept more than 0.4 nC for 12 hours. This value corresponding to the injected rate of 6.1 mA/minute in the case of extraction efficiency = 30%, injection efficiency = 70% and maximum number of injection in one minute = 13. At the same time, the stored beam current in UVSOR-II storage ring was kept almost constant around 300 mA.

This feed-forward system is now always running during user operations for stabilizing the accelerated charge in the synchrotron.

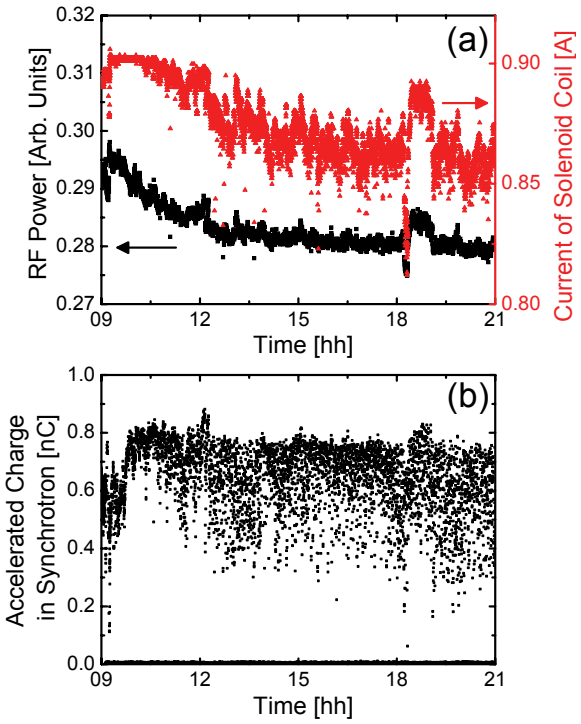

Fig. 2. Temporal evolution of the RF power, excitation current of solenoid coil and accelerated charge in the synchrotron.

[1] H. Zen *et al.*, UVSOR Activity Report **37** (2010) 35.

Stabilization of Pulsed Kickers for Creating Injection Bump Orbit in UVSOR-II Storage Ring

H. Zen, K. Hayashi, J. Yamazaki, M. Adachi and M. Katoh
UVSOR Facility, Institute for Molecular Science, Okazaki 444-8585, Japan

Introduction

Injection of UVSOR-II storage ring is done with three pulsed dipole magnets (kickers) and creating bump orbit near the injection point. The height and timing of those kickers have large drift. Such large drift changes the amplitude of bump orbit, which causes decreasing of injection efficiency or electron beam dump. For stable top-up operation of UVSOR-II, the amplitude of bump orbit should be stabilized. Therefore a feedback system to stabilize the pulsed kickers was developed.

Feedback System

Figure 1 shows the schematic diagram of the developed feedback system. By using an oscilloscope, the excitation current signals of the bump kickers are measured as shown in Fig. 2. The oscilloscope is triggered with an external trigger which generated by a digital delay generator (DG535). We set a threshold level to determine the timing of the kicker and recognized that the operational timing of the kicker is the timing when the current waveform crossing the threshold level as shown in Fig. 2. And the pulse height of the kicker is recognized as the maximum value of the waveform as shown in Fig. 2. In the control PC, measured timing and amplitude are compared with ordered timing and amplitude which are given by machine operators. Based on PID algorithm, the control PC calculates the optimum delay and charging voltage of the kicker. Those values are sent to DG535 and power supply of the kicker.

Since the oscilloscope and DG535 have 4 channels, three bump kickers are controlled by one oscilloscope, one DG535 and one control PC at the same time.

Results

Figure 3 shows the result of feedback control. By properly changing the control value of charging voltage of power supply of the kicker and delay of trigger signal of the kicker, we succeeded in stabilizing the pulse height and operational timing of the kicker.

Though the height and timing of all kickers are stabilized, the injection efficiency of the UVSOR-II ring is not so stable. To keep high injection efficiency, we should slightly vary the strength of steering and focusing magnets of beam transport line between the ring and injector. Counter measures for the fluctuation will be developed near future.

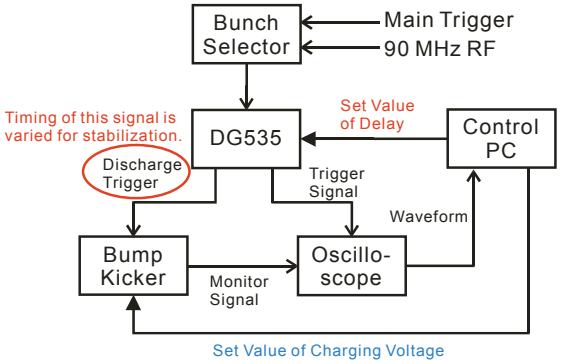

Fig. 1. Schematic diagram of the developed feedback system.

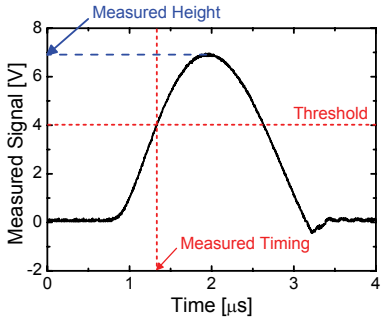

Fig. 2. Typical waveform of excitation current of a pulsed kicker.

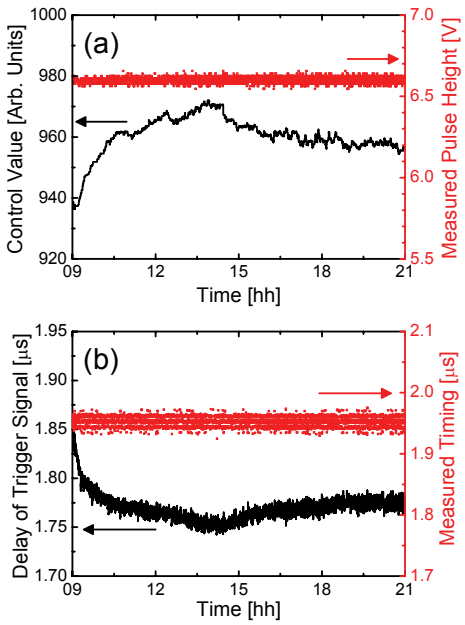

Fig. 3. Temporal evolution of operational condition of a pulsed kicker, (a) control value of charging voltage of the kicker and measured pulse height, (b) delay of discharge trigger signal and measured operational timing of the kicker.

Timing Stabilization of Extraction Kicker of UVSOR-II Injector

H. Zen, K. Hayashi, M. Adachi, J. Yamazaki and M. Katoh
UVSOR Facility, Institute for Molecular Science, Okazaki 444-8585, Japan

Introduction

From this fiscal year, we have started top-up operation of UVSOR-II storage ring during all user operation. In usual operation, 14 buckets of UVSOR-II storage ring are filled by electrons and remained 2 buckets are empty in order to prevent instability caused by ion trapping in the ring [1]. For keeping 2 empty buckets during long time top-up operation, we developed a feedback system for stabilizing the timing of extraction kicker of UVSOR-II injector.

Extraction Scheme and Problem

A fast kicker and an extraction septum are used for extracting electron bunches from UVSOR-II injector, 750 MeV booster synchrotron. At first, the fast kicker suddenly changes the electron beam orbit in the injector. Then 4 bunches in 8 circulating bunches are successfully injected to the extraction septum. Those bunches are bent in the septum and transported to the ring. For filling 14 buckets of the storage ring, the timing of the fast kicker is properly controlled. Although the trigger signal sent to the fast kicker is well controlled, the operational timing of the kicker has long term drift of larger than 40 ns, which corresponds to time interval of 4 buckets. To reduce the drift, a feedback system was developed.

Developed Feedback System

The diagram of the feedback system is shown in Fig. 1. By using an oscilloscope, the excitation current signals of the fast kicker are measured as shown in Fig. 2. The oscilloscope is triggered with the external trigger which generated by a digital delay generator (DG535). We set a threshold level to determine the timing of the kicker and recognized that the extraction timing of bunches is the timing when the current waveform crossing the threshold level as shown in Fig. 2. In control PC, the extraction timing is compared with the ordered timing which is given by machine operators. The control PC calculates the optimum delay of DG535 based on PID algorithm, and sends commands to set the timing delay of DG535 to the calculated delay.

Results

Figure 3 shows the result of feedback control. The fast kicker timing was stabilized around 90 ns, which was the ordered timing of this operation. Then the timing jitter was around 3 ns in FWHM. Figures 4 show the waveforms of bunch pick-up signal after 12-hour top-up operation. As shown Fig. 4 (a), all buckets were filled by electrons without the feedback system. In contrast, we succeeded in keeping the 2 empty buckets with the feedback system as shown in Fig. 4 (b).

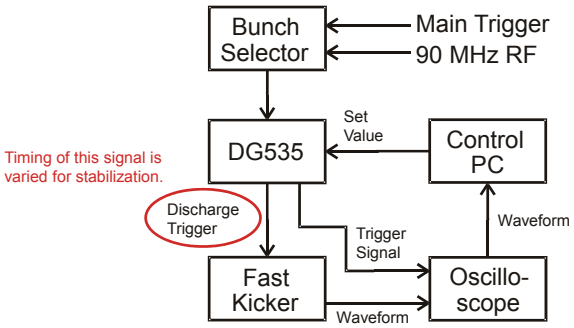

Fig. 1. Diagram of the timing feedback system for the fast kicker.

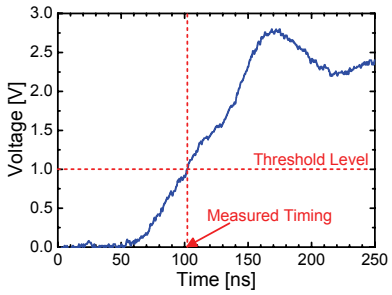

Fig. 2. Way to determine the operational timing of the fast kicker.

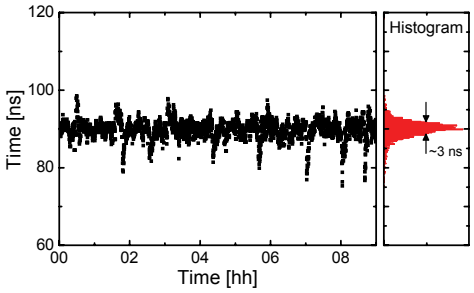

Fig. 3. Temporal evolution of operational timing of fast kicker with developed timing feedback system.

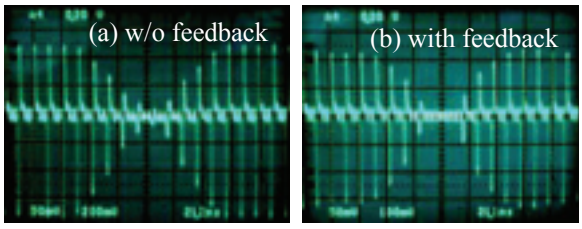

Fig. 4. Photographs of an analog oscilloscope showing an electron bunch pick-up signal after 12-hour top-up operation without (a) and with (b) the timing feedback for the fast kicker.

[1] J. M. Byrdt *et al.*, SLAC-PUB-7389 (1996).

Experiments on the Narrowband Coherent Synchrotron Radiation

M. Hosaka[1], Y. Takashima[1], C. Evain[2], C. Szwaj[2], S. Bielawski[2], M. Shimada[3], A. Mochihashi[4], Y. Takahashi[5], S. Kimura[6] and M. Katoh[6]

[1]*Graduate School of Engineering, Nagoya University, Nagoya 464-8603, Japan*
[2]*Université des Sciences et Technologies de Lille, Villeneuve d'Ascq Cedex, France*
[3]*High Energy Accelerator Research Organization, KEK, Tsukuba 305-0801, Japan*
[4]*Japan Synchrotron Radiation Research Institute (JASRI), SPring-8, Sayo-cho, Hyogo 679-5198, Japan*
[5]*Research Reactor Institute, Kyoto University, Osaka 590-049, Japan*
[6]*UVSOR Facility, Institute for Molecular Science, Okazaki 444-8585, Japan*

Narrowband terahertz coherent synchrotron radiation can occur from an electron bunch whose longitudinal distribution is sinusoidaly modulated. We have already demonstrated this by creating the modulation using interaction inside an undulator between the electron beam and laser pulse containing a sinusoidal amplitude modulation: the resulting narrowband terahertz spectra were observed using a Martin-Pupplett Fourier transform far infra-red spectrometer [1]. In this paper, we report a detail study on the emission, focusing on the efficiency dependence on modulation (or resulting coherent synchrotron radiation) frequency and laser power.

The experimental setup is the same as that we used previously [1], but we simplify the laser pulse shaping system. Instead of using a pair of gratings to achieve dispersion, we extract the pulse of our regenerative amplifier just before the compressor, and send it to a Michelson interferometer. The major improvement over the previous system is higher pulse energy and wider tuning range of the modulation frequency.

To investigate the efficiency dependence of the coherent terahertz emission on the modulation frequency, we recorded the emission intensity as a function of the modulation frequency by changing the Michelson interferometer position. At the same time, we measured the spontaneous synchrotron radiation spectrum using the same setup in order to take into account the frequency dependence of the detecting system. The relative efficiency is deduced dividing the frequency response by the spontaneous synchrotron radiation spectrum. The result is presented in Fig.1. The broad 20 cm^{-1} peak structure agrees well to theoretical calculations based on a slowly-varying envelope approximation [2]. The low frequency emission (around 3-5 cm^{-1}) is attributed to emission after long transport of the storage ring (one full turn and more).

To investigate the efficiency dependence the coherent terahertz emission on the laser power, we attenuated the laser using a half-wave plate followed by a polarizer. By rotating the half-wave plate, we obtained the dependence of terahertz power with incident laser power [Fig. 2]. This dependence appears to be quadratic with good approximation. The quadratic scaling is generally expected in the limit of low laser powers [2]. However, at higher laser power departure from the scaling law is theoretically prospected [2]. As a next step of this study, we are going to examine the behavior with higher laser energy.

[1] S. Bielawski, *et al*., Nature Physics **4** (2008) 390.
[2] C. Evain, *et al*., Phys. Rev. ST Accel. Beams **13** (2010) 090703.

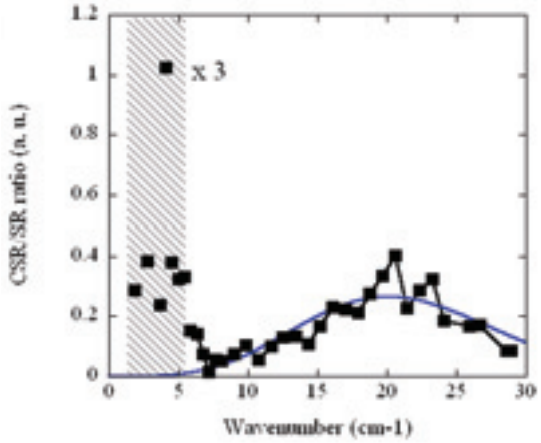

Fig. 1. Ratio between CSR and spontaneous SR versus modulation wavenumber. The blue solid line is theoretically deduced form factor.

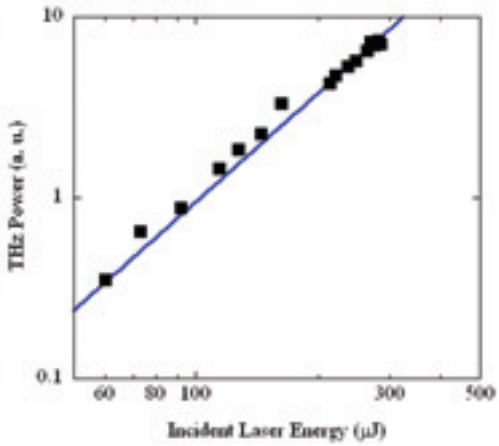

Fig. 2. Terahertz energy versus laser pulse energy. The blue solid line is quadratic law fit.

Generation of Energy-Tunable Gamma Rays via Inverse Compton Scattering in an Electron Storage Ring

Y. Taira[1], M. Adachi[2,3], H. Zen[2,3], T. Tanikawa[3], N. Yamamoto[1], M. Hosaka[1], Y. Takashima[1], K. Soda[1] and M. Katoh[1,2,3]

[1]*Graduate School of Engineering, Nagoya University, Nagoya 464-8603, Japan*
[2]*UVSOR Facility, Institute for Molecular Science, Okazaki 444-8585, Japan*
[3]*School of Physical Sciences, the Graduate University for Advanced Studies, Okazaki 444-8585, Japan*

Gamma rays in the MeV-region can be generated via inverse Compton scattering of laser photons with a relativistic electron beam of sub-GeV or GeV circulating in an electron storage ring. This technology is called laser Compton scattering (LCS) [1]. LCS gamma rays are tunable in energy, quasi-monochromatic, intense, and high polarized, and are used in nuclear science, positron generation, and electron beam diagnosis.

The methods available for tuning the energy of LCS gamma rays include 1) selecting electron beam energy, 2) selecting the laser wavelength, 3) choosing the scattering angle of the gamma rays using a collimator and an absorber, and 4) controlling the collision angle between a laser and an electron beam. Since LCS experiments were usually carried out at electron storage rings operated with fixed electron energy, method 1) cannot be applied to generate LCS gamma rays of tunable energy.

Ohgaki *et al.* [2] performed analytic calculations and computer simulations on the energy spread and intensity of LCS gamma rays using methods 2) - 4) for a 1.4-GeV electron storage ring. The energy spreads obtained using methods 2) and 4) (1 %) were smaller than the spread obtained using method 3) (7-9 %), and the intensity obtained using method 3) (~ 10^5 photons s^{-1}) was the highest of the three. However, the intensity obtained from method 4) is expected to be increased to ~ 10^6 photons s^{-1} when a mode-lock pulse laser was used. Thus Ohgaki *et al.* concluded that method 4) with a mode-lock laser was preferable for generating gamma rays of continuous tunable energy using a laser of fixed wavelength with fixed electron energy.

However, method 4) has never been studied experimentally because LCS gamma rays are usually generated via head-on collision between the electron beam and the laser by injecting the laser through an optical port used for extracting synchrotron radiation. To generate gamma rays of tunable energy using method 4), we installed an optical port in the electron storage ring UVSOR-II which a laser can be injected from the vertical direction with an adjustable collision angle.

Laser pulses of 2.0 W power were provided by a Ti:Sa laser system (COHERENT, LEGEND-HE) synchronized with an RF frequency of the storage ring, 90.1 MHz. The wavelength and the frequency of the laser were 800 nm and 1 kHz, respectively. Gamma rays were detected by an NaI scintillator (1600 cm^3), and the absorption energy was measured.

Experimental data of the absorbed energy spectrum for various collision angles are shown in Fig. 1. Maximum gamma-ray energy and intensity varied in a range from 4 to 9 MeV and from 350 to 850 photons s^{-1}, respectively. It was successfully demonstrated for the first time that the energy of the gamma rays could be tuned by changing the collision angle.

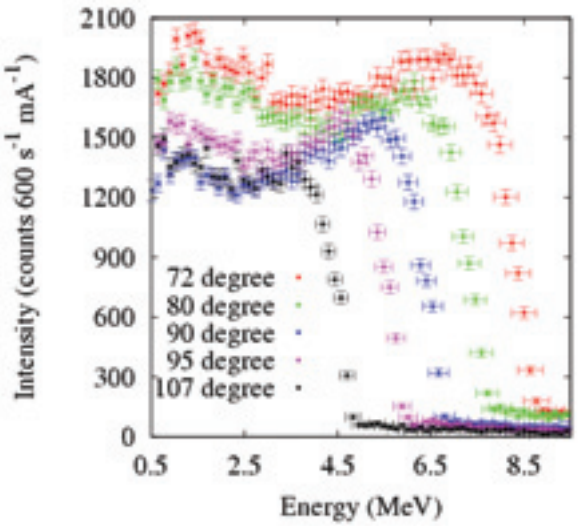

Fig. 1. Experimental data of the energy spectrum for each collision angle listed in the figure. Intensity was standardized by the beam current values. Measurement data of every 100 channels were summed. Error bars in the vertical and horizontal directions are statistical error and energy calibration error, respectively.

[1] J. Stepanek, Nucl. Instr. and Meth. A **412** (1998) 174.
[2] H. Ohgaki, *et al.*, J. Nucl. Sci. and Tech. **44** (2007) 698.

Saturation Phenomena on Coherent Harmonic Generation at UVSOR-II

T. Tanikawa[1], M. Adachi[1,2], H. Zen[1,2], M. Hosaka[3], N. Yamamoto[3], Y. Taira[2,3], J. Yamazaki[2] and M. Katoh[1,2,3]

[1]*The Graduate University for Advanced Studies, Okazaki 444-8585, Japan*
[2]*UVSOR Facility, Institute for Molecular Science, Okazaki 444-8585, Japan*
[3]*Graduate School of Engineering, Nagoya University, Nagoya 464-8603, Japan*

Coherent harmonic generation (CHG) is a method for producing high-order harmonics of a laser light by using a relativistic electron beam. This electron beam interacts with the laser in a sinusoidal magnetic field of an undulator, resulting in microbunching of the electrons at the laser wavelength and in the emission of coherent harmonics (CHs) with a fully coherence, an ultrashort pulse, and a variable polarization [1].

As results of measuring CH spectra by using a vacuum ultraviolet spectrum measurement system constructed in last year at UVSOR-II [2], they have been observed up to 9th harmonic. Figure 1 shows the intensities of the 5th, 7th, and 9th CHs as functions of the peak laser power. Figure 2 shows the intensity of the 5th CH over a wide range of peak laser powers. Dots in Fig. 1 and Fig. 2 represent measured value. In Fig. 1, the CH intensities increase with increasing the peak laser power, reaching a maximum at a value of the power that decreases slightly with the order of the CH. In Fig. 2, the CH intensity oscillates after the maximum.

The dashed and solid curves in Fig. 1 and 2 represent the results of a one-dimensional analytical calculation based on a simple equation for the form factor at each harmonics [3]. The calculation on dashed curve assumes that the longitudinal distribution of the laser is uniform, and that on solid curve assume that the distribution is a Gaussian. As shown in Fig. 1, the calculations reproduced the observed variation in the width and position of the intensity peak for the three harmonics. The peak position shifts to lower peak laser powers with increasing order of the CH. Fig. 2 shows that calculations also reproduced several other peaks observed in the deep saturation regime qualitatively. To understand these results, we carried out a one-dimensional particle tracking simulation of the bunching process in the saturated regime. In Fig. 1, in the case of higher-order CHs, the Fourier component of a longitudinal distribution on the electron beam is largest near the optimal bunching condition, where the bunching is sharpest. However, for lower-order CHs, the Fourier component is largest when the electrons are slightly overbunched because of the contribution of more electrons. For this reason, the lower-order CHs reach their maximum intensity at larger peak laser power. In Fig. 2, the experiments and simulations show several peaks appearing beyond the first maximum, which can be explained by an "additive interference" of the double-peak structure shown in Fig. 3. When the separation of the peaks equals a multiple of the harmonic wavelength, interference produces peaks in the Fourier components, and hence in the CH intensities.

In summary, we have demonstrated that CHG is a useful probe for investigating the formation and evolution of the microbunching caused by laser-electron interactions, which contributes to the next-generation seeded free-electron lasers [4].

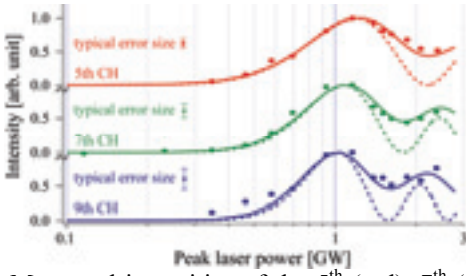

Fig. 1. Measured intensities of the 5th (red), 7th (green), and 9th (blue) CHs plotted as functions of the peak laser power.

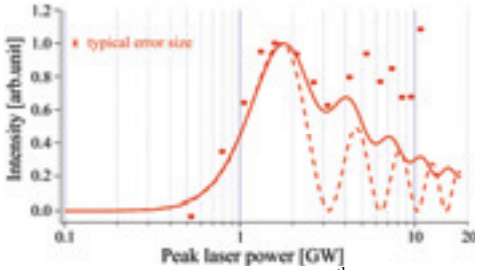

Fig. 2. Measured intensity of the 5th CH plotted as a function of the peak laser power.

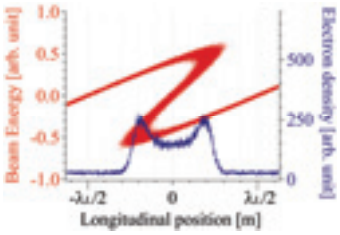

Fig. 3. Simulation result of the bunching process on the overbunching condition in the OK.

[1] M. Labat *et al.*, Phys. Rev. Lett. **101** (2008) 164803.
[2] T. Tanikawa *et al.*, UVSOR Activity Report **37** (2010) 40.
[3] P. L. Csonka, Part. Accel. **11** (1980) 45.
[4] T. Tanikawa *et al.*, Appl. Phys. Exp. **3** (2010) 122702.